DESIGN, ANALYSIS OF BROADBAND VIBRATION ENERGY HARVESTER USING MAGNETOELECTRIC TRANSDUCER

Jin Yang, Yumei Wen*, Ping Li, Xianzhi Dai, Ming Li
The Key Laboratory for Optoelectronic Technology & Systems, Ministry of Education, China
Department of Optoelectronic Engineering, Chongqing University, Chongqing, China
*Presenting Author: ymwen@cqu.edu.cn

Abstract: This paper presents a new broadband vibration energy harvester using magnetoelectric (ME) transducer. The harvester using ME transducer takes advantage of multi-cantilever beams and nonlinear behavior of the magnetic force to expand the working bandwidth in ambient low frequency vibration. A theoretical model is developed to analyze the nonlinear vibration of the harvester, and the effects of the structure parameters on the electrical-output and the bandwidth of the harvester are analyzed to achieve the optimal vibration energy harvesting performances. The experimental results on the performances show that, the harvester has bandwidths of 5.2Hz, 6.3Hz, and 7.2Hz at the accelerations of 0.2g, 0.4g, and 0.6g(with $g=9.8ms^{-2}$), respectively.

Keywords: energy harvesting, magnetoelectric transducer, wide-spectrum vibration, nonlinear magnetic force

INTRODUCTION

The demand for energy harvesting devices has been growing rapidly with the wide application of mobile electronics and wireless sensors. Mechanical energy associated with vibration has been one of the major energy sources for energy harvesting systems. Different vibration energy harvesting mechanisms have been utilized, including piezoelectric [1], electromagnetic [2], electrostatic [3], or ME transduction mechanisms [4-7].

Regardless of the transduction mechanism, a primary issue in vibration-based energy harvesting is that the best performance of a harvester is usually limited to excitation at its fundamental resonance frequency. If the applied ambient vibration deviates slightly from the resonance condition then the power out is drastically reduced. In order to solve this problem, several solutions have been proposed in the literature like active/passive frequency tuning techniques [8–12] and widening of the bandwidth techniques [13-16]. In active/passive tuning techniques, simply the parameters of the harvester such as the mass or the stiffness are altered so that the resonance frequency is tuned to match the environmental vibration frequency. In the active tuning technique, this adjustment is done continuously, whereas in the case of passive tuning technique, the tuning actuators turn off after the adjustment. Roundy and Zhang [12] mathematically showed with some assumptions that active tuning techniques were not feasible because the tuning actuators required more power than the device could generate. On the other hand, passive tuning techniques also require actuators and sensors, which increase the complexity and the cost of the device. Another solution is to widen the bandwidth of the harvester. The reported generators covered a wide band of external vibration frequency by implementing a number of serially connected cantilever beams with varying natural frequencies [13-14]. Nonlinear behavior offers new capabilities to capture energy available from more complex excitations, and several recent papers demonstrated the efficacy of this approach [15-16]. These broadening technologies in the harvesters using piezoelectric, electromagnetic and electrostatic transduction mechanisms have shown some promise, but they can not be applied in the harvesters using ME transducers directly due to the different transduction mechanisms.

This paper presents a new broadband vibration energy harvester using ME transducer to expand the working bandwidth in ambient low frequency vibration.

HARVESTER DESIGN AND MODELING

Fig. 1 shows the schematic diagram of the proposed vibration energy harvester. The harvester consists of two cantilever beams, a magnetic circuit, and a ME transducer. The magnetic circuit is made of four rectangular NdFeB magnets and two magnetic yokes, and is placed on the end of the cantilever beam B and acts as the proof mass. The four magnets are arranged in multi-pole, head-to-head arrangement to generate a concentrated flux gradient. The ME transducer is a sandwich of one piezoelectric layer bonded between two magnetostrictive layers, and is placed at the tip of the cantilever beam A and acts as the proof mass. The beams A and B are both fixed to the housing of the harvester.

The two cantilever beams are initially designed to have different natural frequencies. If the source frequency matches the resonant frequency of one of the cantilever beams (with magnetic coupling), the acceleration due to the external vibration will cause relative motion between the ME transducer and the magnetic circuit. The ME transducer undergoes magnetic field variations in the air gap among the four magnets. In turn, the changing magnetic field causes the magnetostrictive layers to generate stress. The stress is then transmitted to the piezoelectric layer, which generates electrical power.

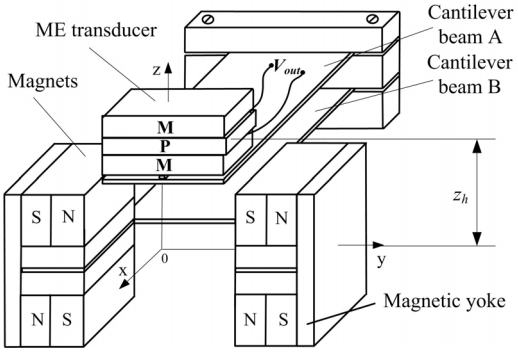

Fig.1: Schematic diagram of the proposed vibration energy harvester.

The governing equations for the 2DOF harvester are given by

$$\mathbf{M}\ddot{\mathbf{Z}} + \mathbf{C}\dot{\mathbf{Z}} + \mathbf{K}\mathbf{Z} = \mathbf{F_A} + \mathbf{F_M} \tag{1}$$

where, $\mathbf{M} = \begin{bmatrix} m_A & 0 \\ 0 & m_B \end{bmatrix}$, $\mathbf{C} = \begin{bmatrix} c_A & 0 \\ 0 & c_B \end{bmatrix}$, $\mathbf{Z} = \begin{bmatrix} z_A \\ z_B \end{bmatrix}$, $\mathbf{K} = \begin{bmatrix} k_A & 0 \\ 0 & k_B \end{bmatrix}$, $\mathbf{F}_A = \begin{bmatrix} m_A\ddot{z}_f \\ m_B\ddot{z}_f \end{bmatrix}$, $\mathbf{F}_M = \begin{bmatrix} F_{MA}(z_A, z_B, z_h) \\ -F_{MB}(z_A, z_B, z_h) \end{bmatrix}$.

m_A and m_B are the masses at the tip of the beam A and the beam B, respectively. The mechanical losses are modeled by the viscous damping factors c_A and c_B. k_A and k_B are the spring constants of the beams A and B, respectively. z_f is the vertical displacement of the frame, and z_A and z_B are the relative displacements of the mass A and the mass B to the frame. F_{MA} and F_{MB} are the z-components of the magnetic forces acting respectively on the mass A and the mass B.

When the ME transducer vibrates under free-free boundary conditions at low frequency (f < 1000 Hz), its magnetoelectric equivalent circuit [17] is as shown in Fig.2. In the equivalent circuit, H_y is the external excitation magnetic field, and $\triangle H_y$ is the induced magnetic field variation; I is the electric current; R_L is the load resistance; α_V is the ME voltage coefficient, and $\alpha_V = \partial V_{\mathrm{ME}}/\partial H_y$ with V_{ME} the induced ME voltage; C is the equivalent capacitance of the ME transducer, which has a capacitive impedance.

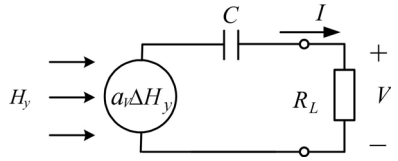

Fig.2: ME transducer equivalent circuit under free-free conditions.

In Fig.2, the output voltage and power across the load resistance R_L are

$$V = \left| \frac{\alpha_V \Delta H_y R_L}{\frac{1}{j\omega C} + R_L} \right| = \frac{\alpha_V \Delta H_y R_L \omega C}{\sqrt{1 + (\omega C R_L)^2}} \tag{2}$$

$$P = \frac{V^2}{R_L} = \frac{(\alpha_V \Delta H_y \omega C)^2 R_L}{[1 + (\omega C R_L)^2]} \tag{3}$$

According to Eq.(3), the optimal load resistance can then be found by differentiating Eq. (3) with respect to R_L, setting the result equal to zero, and solving for R_L. Note that when $R_L = R_{opt}$, the harvester power output is maximum, a condition referred to as impendence matching. In this case the corresponding power is given as

$$P_{\max} = \pi f \alpha_V^2 \Delta H_y^2 C \tag{4}$$

According to Eqs.(2) and (4), in order to achieve a large output voltage and power, the magnet circuit in Fig.1 should provide the ME transducer to work in the best DC magnetic bias field to obtain the optimal ME voltage coefficient α_V, and the ME transducer should undergo large enough magnetic field variation $\triangle H_y$ at a small relative displacement.

The soft of Ansoft's Maxwell 3D is employed to simulate and analyze the magnetic force and the magnetic field. In simulations, the dimension of each magnet in the magnetic circuit is 6 mm×6 mm×2.5 mm. The distance between the upper magnet and the lower magnet is 2.5mm, and that between the left magnet and the right one is 14mm. The remnant flux density (B_r) and the relative permeability (μ_r) of the magnets are 1.39 T and 1.09 T, respectively.

In Eq. (1), because the magnitudes of z_A and z_B are generally small, F_{MA} and F_{MB} are mainly related to the initial distance z_h. Therefore, the frequency characteristics of the beams A and B varying with z_h are analyzed. The magnitude of the corresponding magnetic stiffness, k_{mag}, can be written in terms of the change in magnetic force as a function of distance as [12]

$$k_{mag} = \left| \frac{d(F_{MA}(z_h))}{dz_h} \right| = \left| \frac{d(F_{MB}(z_h))}{dz_h} \right| \tag{5}$$

where the sign of the k_{mag} is dependent on the mode of the magnetic force (i.e. positive for the repulsive magnetic mode and negative for the case of the attractive magnetic mode) [12]. It can be seen that, the effective stiffness of the beam would be smaller or larger than the beam stiffness with no magnetic coupling.

Fig.3 shows the simulation results of the magnetic force F_{MA} by Ansoft's Maxwell for different z_h values, and the corresponding magnetic stiffness k_{mag}. From Fig.3, we can see that, 1) when z_h is changed from 0 to 2.1 mm, the mode of the magnetic force F_{MA} is always repulsive, and the sign of k_{mag} in Eq.(5) is positive. The effective resonant frequency of the beam A will be tuned to be higher than that of the beam with no magnetic coupling. 2) When the initial distance z_h is

beyond 2.1 mm, the mode of the magnetic force F_{MA} is changed to be attractive. The additional stiffness k_{mag} will alter the effective resonant frequency to be lower than that of the beam A (no magnetic coupling) except when z_h is 4.2mm. At z_h=4.2mm, the magnitude of the magnetic force F_{MA} reaches maximum, but the corresponding additional stiffness k_{mag} is zero. As a consequence, the resonant frequency of the beam A will remain unchanged.

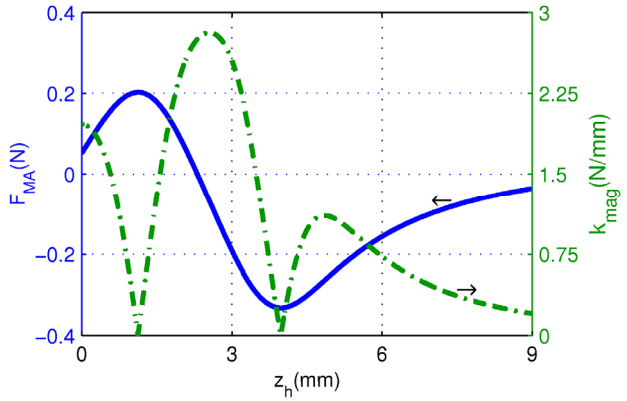

Fig.3: Magnetic force and additional stiffness for different z_h values

Fig.4 plots the average magnetic field along y direction in the air gaps and the corresponding magnetic field variation for different z_h value.

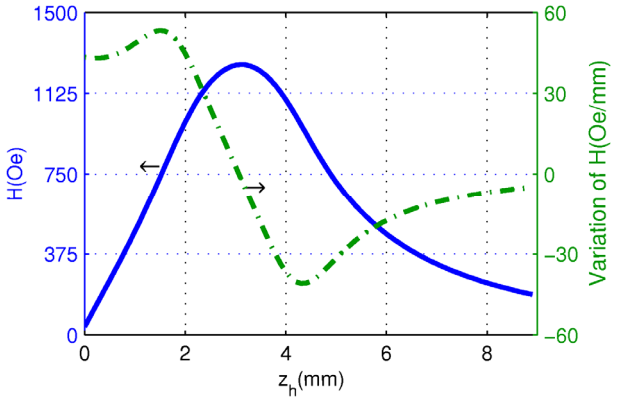

Fig.4: Magnetic field along y direction and variation

As can be seen from Fig. 4, the curve of the magnetic field variation presents two peaks at z_h= 1.7 mm and 4.2 mm, and the absolute peak values reach 55Oe/mm and 41Oe /mm, respectively. These two distances (z_h= 1.7 mm and 4.2 mm) may be used as the optimal initial position to place the ME transducer, if the ME transducer can work in the best condition of the DC bias field at these positions.

EXPERIMENT AND RESULT

Experimental Setup

The cantilever beams are both made up of 10mm×10mm×0.5mm beryllium bronze. The dimensions of NdFeB magnets are 6mm×6mm×2.5mm. The distance between the upper magnet and the lower one is 2.5mm and that between the left magnet and the right one is 14mm. The material of the two magnetic yokes is mild steel. The ME transducer is a sandwich of one PMNT layer (12mm×6mm× 0.8mm) bonded between two Terfenol-D layers (12mm×6mm×1mm). The Terfenol-D layers are magnetized along the longitudinal direction, and the piezoelectric layer is polarized in its thickness direction.

Fig.5 shows the experimental set-up. A vibration shaker is used to supply mechanical vibrations to the prototype and an amplifier is used to drive the shaker. An accelerometer is mounted in the vibration shaker to measure the acceleration of vibrations applied to the prototype. The output voltage of the prototype is measured and stored by a Tektronix TDS2022B digital storage oscilloscope. In all measurements, the shaker table acceleration is set to 0.2g.

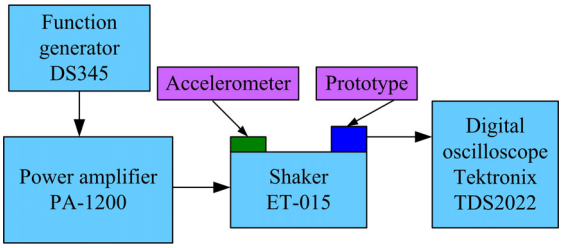

Fig. 5: Experimental setup

Experimental Result

The ME transducer is placed at the end of the beam A with the natural frequency of 37.5Hz. The beam B with the magnetic circuit has the natural frequency of 41.5Hz. In addition, the beam B is fixed on a clamp that can be vertically displaced using a screw–spring mechanism to change the initial distance z_h. Fig. 6 plots the measured open-circuit voltages versus frequency for three different values of z_h.

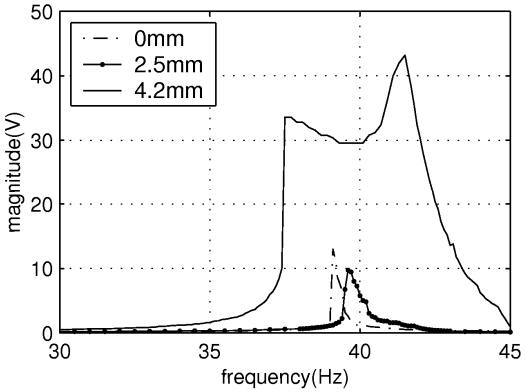

Fig. 6: Output voltages versus frequency for different z_h values

In Fig.6, it can be seen that: 1) when z_h is in the range of 0 to 2.5 mm, there is only one peak in the frequency response of the harvester, and the value of the resonant frequency is between that of the two beams. 2) When z_h=4.2mm, because the additional stiffness k_{mag} is zero, the resonant frequencies of the beam A and the beam B are unchanged and are equal to the corresponding natural frequencies, respectively.

Further, by nonlinear behavior of the magnetic force, both hardening and softening responses of the beams A and B appear in Fig.6, which allow the frequency response to be broadened in either direction [16]. And the resonance peaks of the two beams overlap to successfully widen the bandwidth of the harvester. In this case, the harvester shows a 3dB bandwidth of 5.2Hz.

Considering the output voltages and the bandwidths for different z_h, we think that the output performance of the harvester is optimal when z_h=4.2mm. Fig. 7 plots the measured open-circuit voltages at three accelerations when z_h=4.2mm. It can be seen that, the output voltage and the bandwidth of the harvester increase with increasing the acceleration. The bandwidths of the harvester are 5.2Hz, 6.3Hz, and 7.2Hz at the accelerations of 0.2g, 0.4g, and 0.6g, respectively.

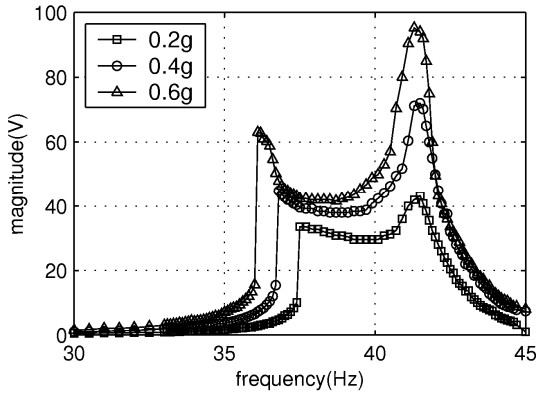

Fig. 7: Output voltages versus acceleration

CONCLUSION

This study presents a new broadband vibration energy harvester using ME transducer. The experimental results on the performances show that, the harvester has bandwidths of 5.2Hz, 6.3Hz, and 7.2Hz at the accelerations of 0.2g, 0.4g, and 0.6g, respectively.

ACKNOWLEDGMENTS

This work was supported by the National Natural Science Foundation of China (61071042, 10776039, 50830202)

REFERENCES

[1] Roundy S 2004 A piezoelectric vibration based generator for wireless electronics *Smart Mater. Struct*. **13** 1131

[2] Buren T von, Mitcheson P D, Green T C, Yeatman E M, Holmes A S, Troster G 2005 Optimization of inertial micropower generators for human walking motion *IEEE Sensors J.* **99** 1–11

[3] Kuehne I, Frey A, Marinkovic D, Eckstein G, and Seidel H 2008 Power MEMS-A capacitive vibration-to-electrical energy converter with built-in voltage *Sens. Actuators: A* **142** 263–269

[4] Huang J, O'Handley R C, Bono D 2003 New, high-sensitivity, hybrid magnetostrictive/ electroactive magnetic field sensors *Proc. SPIE*, **5050** 229–237

[5] Bayrashev A, Robbins W P, Ziaie B 2004 Low Frequency Wireless Powering of Microsystems Using Piezoelectric-magnetostrictive Laminate Composites *Sens. Actuators: A* **114(2-3)** 244–249

[6] Wang L, Yuan F G 2008 Vibration energy harvesting by magnetostrictive material *Smart Mater. Struct.* **17** 045009

[7] Dai X Z, Wen Y M, Li P, Yang J, Zhang G Y 2009 Modeling, characterization and fabrication of vibration energy harvester using Terfenol-D/PZT/Terfenol-D composite transducer, *Sens. Actuators: A* **156(2)** 350-358

[8] Leland E S, Wright P K 2006 Resonance tuning of piezoelectric vibration energy scavenging generators using compressive axial preload *Smart Mater. Struct.* **15** 1413–1420

[9] Morris D J, Youngsman J M, Anderson M J, Bahr D F 2008 A resonant frequency tunable, extensional mode piezoelectric vibration harvesting mechanism *Smart Mater. Struct.* **17** 065021

[10] Challa V R, Prasad M G, Shi Y, Fisher F T 2008 A vibration energy harvesting device with bidirectional resonance frequency tenability *Smart Mater. Struct.* **17** 015035

[11] Christian P, Dominic M, Wolfram S, Florian M, Yiannos M 2009 A closed-loop wide-range tunable mechanical resonator for energy harvesting systems *J. Micromech. Microeng*. **19** 094004

[12] Roundy S, Zhang Y 2005 Toward self-tuning adaptive vibration based microgenerators *Proc. SPIE* **5649** 373–384

[13] Sari I, Balkan T, Kulah H 2008 An electromagnetic micro power generator for wideband environmental vibrations *Sens. Actuators: A* **145–146** 405–413

[14] Liu J Q, Fang H B, Xu Z Y, Mao X H, Shen X C, Chen D, Liao H, Cai B C 2008 A MEMS-based piezoelectric power generator array for vibration energy harvesting *Microelectron. J.* **39(5)** 802-806

[15] Stanton S C, McGehee C C, Mann B P 2009 Reversible hysteresis for broadband magneto-piezoelastic energy harvesting *Appl. Phys. Lett.* **95** 174103

[16] Erturk A, Hoffmann J, Inman D J 2009 A piezomagnetoelastic structure for broadband vibration energy harvesting *Appl. Phys. Lett.* **94** 254102

[17] Bian L X, Wen Y M, Li P 2009 Composite magnetoelectric transducer of Terfenol-D and Pb(Zr,Ti)O3 plates bonded on an elastic substrate *IEEE Sensors J.* **9(1)** 45–50